Organic & Biomolecular Chemistry

Accepted Manuscript

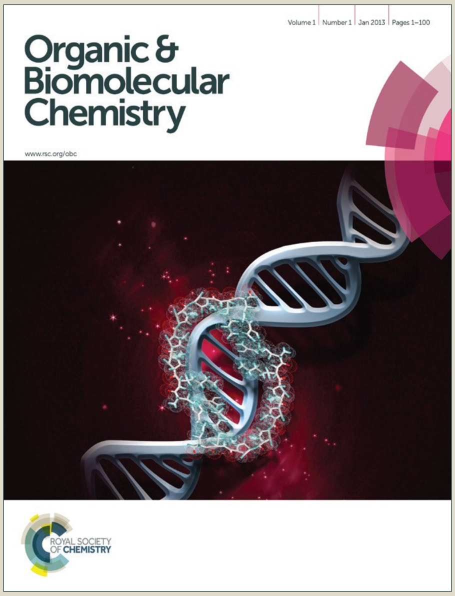
Volume 1 | Number 1 | Jan 2013 | Pages 1–100
Organic & Biomolecular Chemistry
www.rsc.org/obc
ROYAL SOCIETY OF CHEMISTRY

This is an *Accepted Manuscript*, which has been through the Royal Society of Chemistry peer review process and has been accepted for publication.

Accepted Manuscripts are published online shortly after acceptance, before technical editing, formatting and proof reading. Using this free service, authors can make their results available to the community, in citable form, before we publish the edited article. We will replace this *Accepted Manuscript* with the edited and formatted *Advance Article* as soon as it is available.

You can find more information about *Accepted Manuscripts* in the Information for Authors.

Please note that technical editing may introduce minor changes to the text and/or graphics, which may alter content. The journal's standard Terms & Conditions and the Ethical guidelines still apply. In no event shall the Royal Society of Chemistry be held responsible for any errors or omissions in this *Accepted Manuscript* or any consequences arising from the use of any information it contains.

ROYAL SOCIETY
OF **CHEMISTRY**

www.rsc.org/obc

Journal Name

RSCPublishing

COMMUNICATION

Cell-Targeted Platinum Nanoparticles and Nanoparticle Clusters

Cite this: DOI: 10.1039/x0xx00000x

Stefanie Papst,[a] Margaret A. Brimble*,[a] Clive W. Evans,[c] Daniel J. Verdon,[c] Vaughan Feisst,[c] Rod P. Dunbar,[c] Richard D. Tilley,[b] and David E. Williams*[a]

Received 00th January 2012,
Accepted 00th January 2012

DOI: 10.1039/x0xx00000x

www.rsc.org/

Herein, we report the facile preparation of cell-targeted platinum nanoparticles (PtNPs), through the design of peptides that, as a single molecule added in small concentration during the synthesis, control the size of PtNP clusters during their growth, stabilise the PtNPs in aqueous suspension and enable the functionalisation of the PtNPs with a versatile range of cell-targeting ligands. Water-soluble PtNPs targeted respectively at blood group antigens and at integrin receptors are demonstrated.

Over the past decades, research in the field of monolayer-protected metal nanoparticles (NPs) has been extremely active. Combining the unique physicochemical properties of particles at the nanoscale with a tightly packed layer of organic species has enabled access to hybrid materials with superior properties for a wide range of applications such as catalysis, biomedicine and imaging.[1, 2, 3] Metal NPs with a high atomic number of the material, Pt in particular, have been used as both imaging and anti-cancer agents. Thus, gold NPs (AuNPs) and platinum NPs (PtNPs), exhibit greater X-ray attenuation than other commonly used computed tomography (CT) contrast agents. They have the potential to significantly improve CT imaging applications permitting imaging at lower radiation doses and with better sensitivity compared to the currently used iodine-based contrast agents.[4] Recently, the combination of fast ion radiation (hadron therapy) with PtNPs as high-Z sensitising agents has been suggested by Porcel *et al.* as a route towards strongly improved cancer radiation therapy protocols.[5] Furthermore, PtNPs possess significant cell toxicity and also anti-oxidative and anti-inflammatory capacity and have therefore been recommended for new anticancer approaches,[6] for treatment of bone loss,[7] and for medical treatment of diseases related to oxidative stress and ageing.[8] They usually eliminate the need for attaching anticancer drugs to kill cancer cells due to their inherent toxicity.[9] Teow *et al.*, for example, prepared folic acid-conjugated PtNPs that induced significant reduction in viability of cancer cell lines which over-express folate receptors on their surfaces.[6]

Being able to target PtNPs efficiently to specific cell surface receptors is of paramount importance for their utility as cytotoxic or imaging agents. Peptides selected by combinatorial phage display or cell-surface display methods from large libraries of random sequences have been used successfully for the synthesis of platinum nanocrystals with very good size and shape control.[10] However, these methods identify sequences with the greatest affinity for the inorganic target, but such sequences are not optimal for the intended application such as receptor targeting of the NPs. Dried leaf powders, fungi, chaperone proteins and other protein shells have been used as capping agents for the one-step preparation of targeted PtNPs.[11] Using these procedures, however, greatly limits the range of applications, because the size and shape of the PtNPs is controlled by the targeting ligand i.e. changing the targeting ligand will alter the size and shape of the PtNPs.

The aim of the present study was to access *via* a simple two-step method PtNPs targeted at a versatile range of receptors while retaining size control. Firstly, water-soluble PtNPs were prepared in one step by reducing K_2PtCl_6 in the presence of a small amount of a specifically designed peptide and subsequently different cell-targeting ligands were attached to the amine-reactive carboxyl groups of the peptides using EDC/ sulfo-NHS activation.[12] It was expected that the attachment of cell-targeting ligands containing multiple amino groups would lead to the formation of crosslinked PtNP-ligand clusters (**Fig. 1**, top), whereas the attachment of ligands containing only one amino group would lead to the formation of separated ligand-presenting PtNP conjugates (**Fig. 1**, bottom).

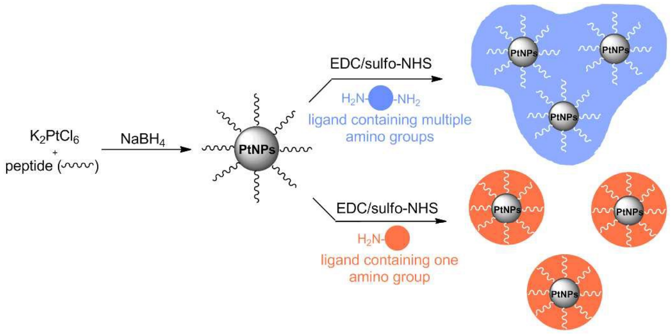
K2PtCl6
+
peptide
NaBH4
PtNPs
EDC/sulfo-NHS
H2N- -NH2
ligand containing multiple amino groups
EDC/sulfo-NHS
H2N-
ligand containing one amino group
PtNPs

Fig. 1 Two-step synthesis of crosslinked PtNP-ligand clusters (top) and separated PtNP-ligand conjugates (bottom) mediated by rationally designed peptides.

In 2004, Lévy *et al.* published the design of the pentapeptide CALNN, which converts pre-formed, citrate-stabilised AuNPs into extremely stable, water-soluble AuNPs.[13] For this study, the N-terminal cysteine residue was replaced with histidine leading to the peptide sequence HALNN, which was expected to have strong affinity for platinum due to the presence of the imidazole ring adjacent to the N-terminus.[14] Indeed, stabilisation of Pt nanoparticle clusters by histidine and by the peptide AHHAHHAAD was demonstrated in 2003.[15] We also attached a hexaglutamic acid tag to the C-terminus of HALNN leading to peptide sequence HALNNE$_6$, which was expected to improve the stability of the PtNPs in aqueous suspension by electrostatic stabilisation. Both peptides do not contain any other amino groups except the platinum-bound N-termini. This will enable the controlled covalent attachment to the carboxyl functions contained in HALNN and HALNNE$_6$ of a diverse range of receptor-targeting ligands *via* their amino groups. Hence, the peptides served three purposes: they were used (a) as capping agents for the one-step preparation of water-soluble PtNPs, (b) as stabilising agents in aqueous suspension and (c) as linkers between the PtNPs and the biologically-targeting ligands.

Peptide HALNN was synthesised manually using standard Fmoc solid-phase peptide synthesis (SPPS) with the C-terminal asparagine being introduced into the sequence by attachment of N^{α}-Fmoc-C^{α}-*tert*-butyl aspartate to Rink amide linker via the unprotected ω-carboxyl group. This synthesis protocol significantly increases peptide yield and helps avoid ω-side chain dehydration and imide formation (α → ω rearrangement) of the asparagine residue (ESI, section 1.2).[16] Peptide HALNNE$_6$ was synthesised using a Tribute peptide synthesiser and standard Fmoc SPPS on aminomethylated polystyrene (PS) resin (ESI, section 1.3). Chain elongations proceeded normally and acid cleavage released the desired peptides in high yield and purity. The PtNP synthesis protocol was simply the reduction of K_2PtCl_6 by $NaBH_4$ in water at RT in the presence of a small amount of the respective peptide affording very stable aqueous colloidal suspensions of the generated PtNPs-HALNN(E$_6$) conjugates that were essentially indefinitely stable (months) and could be centrifuged, dried and resuspended for analysis (ESI, sections 1.6-1.8). In the absence of the peptide the PtNPs started precipitating after about 2 days presumably because the particles are stabilised to a degree by chloride adsorption. Transmission electron microscopy (TEM) images showed that the PtNPs-HALNN conjugates are joined spherical nanocrystals with an average diameter of 2.8 (± 0.4) nm (ESI, Fig. S8-10). Dynamic light scattering (DLS) experiments revealed that in aqueous solution they form aggregates with an average hydrodynamic diameter of about 38 nm with a polydispersity index (PDI) of 0.12 before freeze-drying of the sample. After lyophilisation and redispersion in aqueous buffer, however, the average hydrodynamic diameter increased to 154 nm and the PDI to 0.36 indicating that the freeze-drying step led to increased aggregation of the PtNPs-HALNN conjugates (**table 2**, entry 4). It was also observed that PtNPs-HALNN adhered to a certain degree to the surfaces of laboratory plastic equipment such as pipette tips and centrifuge tubes, presumably *via* hydrophobic interactions between the alanine and leucine side-chains of HALNN and the polypropylene surfaces.

TEM analysis of the PtNPs-HALNNE$_6$ conjugates showed that the sample consisted of joined spherical nanocrystals with an average diameter of 3.3 (± 0.8) nm (ESI, Fig. S13-15). DLS analysis of the PtNPs-HALNNE$_6$ conjugates revealed that the sample was relatively monodisperse (PDI = 0.25-0.29) with an average aggregate size of about 180 nm in aqueous suspension before freeze-drying and also after redispersion (**table 2**, entry 5). Furthermore, PtNPs-HALNNE$_6$ suspensions did not adhere to any plasticware used in the laboratory. This indicates that the introduction of the negatively charged E$_6$-tag into the peptide efficiently increased the electrostatic stabilisation of the sample decreasing the interactions of the PtNPs-HALNNE$_6$ conjugates with one another as well as with plastic surfaces (**Fig. 2**).

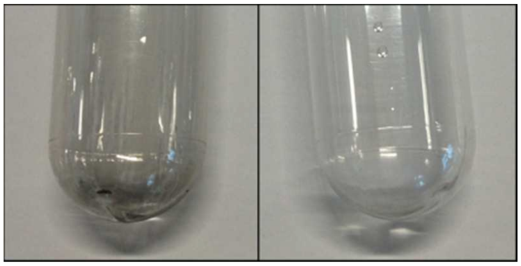

Fig. 2 Ultracentrifuge plastic tubes photographed after spinning EDC/sulfo-NHS-activated PtNPs-HALNN (left) and PtNPs-HALNNE$_6$ (right) at 27,000 rpm (2 h): The addition of the E$_6$-tag successfully suppressed PtNP adhesion to plastic surfaces (right).

High-resolution TEM images showed that both samples were polycrystalline and uniform lattice fringes across the nanocrystals were observed. The most intense rings of the selected area electron diffraction (SAED) patterns of PtNPs-HALNN (ESI, Fig. S12) and PtNPs-HALNNE$_6$ (ESI, Fig. S17) can be indexed to the (111), (200), (220), and (311) reflexions of fcc-Pt. Energy-dispersive X-ray spectroscopy (EDS) analysis confirmed the presence of platinum in both specimens (ESI, Fig. S11 and S16).

It is assumed that the addition of $NaBH_4$ leads to the almost instantaneous formation of Pt(0) nuclei, which rapidly form nanocrystals whose growth rate is reagent diffusion limited and that coalesce into clusters as they form. The cluster growth is stopped by the adsorption of the peptide to the PtNP surface so the cluster size will be dependent on the peptide concentration and diffusion coefficient.[15] The overall larger size of the PtNPs-HALNNE$_6$ conjugates compared to PtNPs-HALNN can be attributed to the smaller diffusion coefficient of peptide HALNNE$_6$ compared to HALNN due to its higher molecular weight.

The second step of the procedure, the attachment of cell-targeting ligands to PtNPs-HALNN conjugates, was demonstrated in a proof-of-concept study. Concanavalin A (ConA) is a homotetrameric plant lectin that strongly agglutinates erythrocytes irrespective of blood groups.[17] Herein, the well-known ConA-induced red blood cell (rbc) aggregation assay was used to confirm the feasibility of the simple one-pot preparation of ConA-functionalised PtNPs-HALNN clusters and their attachment to the blood group antigens of rbcs.

For ConA attachment, a freshly prepared sample of PtNPs-HALNN (ESI, section 1.6) was centrifuged, the reaction mixture was decanted and the NPs were resuspended in PBS buffer containing 6 eq. of EDC and 1.5 eq. of sulfo-NHS to activate the C-termini of the peptides. After incubation for 30 min, the activated PtNPs-HALNN conjugates were centrifuged, washed with PBS buffer to remove 'free' EDC/ sulfo-NHS from the solution, and resuspended in an aqueous solution containing 270 µg of ConA. The reaction mix was shaken at RT for 3 h, then the formed PtNPs-HALNN-ConA **1** clusters were centrifuged and the supernatant decanted. Non-bound protein was removed by washing the clusters thoroughly with PBS buffer using sonication, and subsequently the sample was freeze-dried and stored at -20 °C (ESI, section 1.9). TEM images of the sample showed that the PtNPs-HALNN conjugates were attached to and covered with a large amount of organic material (ESI, Fig. S18). The SAED pattern of **1** is shown in the ESI (Fig. S19). The most intense rings can be indexed to the (111), (200), (220), and (311) reflexions of fcc-Pt. EDS analysis confirmed the presence of platinum in the sample (ESI, Fig. S20) and DLS experiments revealed an increase in size from 38 nm to 427 nm after ConA

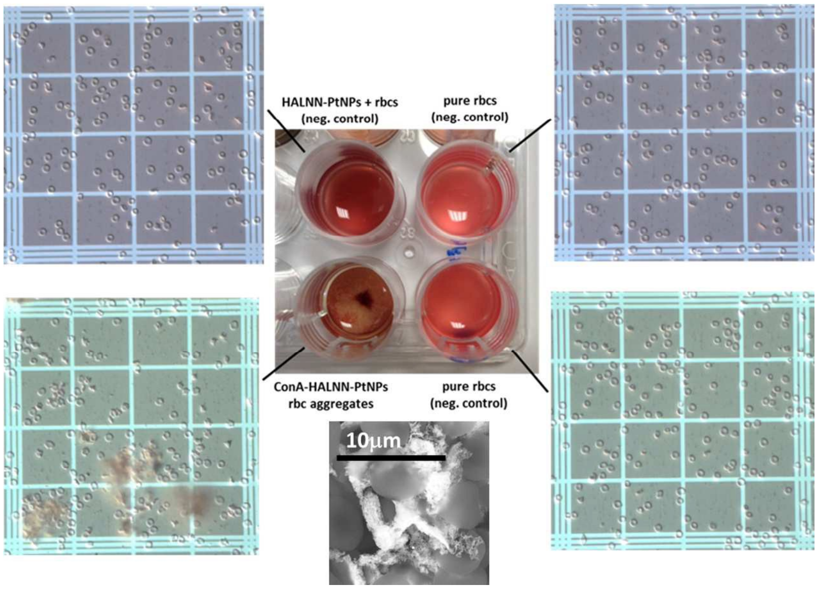

Fig. 3 Rbc aggregation assay demonstrating that only the sample containing PtNPs-HALNN-ConA **1** agglutinated. Samples were deposited on a haemocytometer and images were taken with a digital camera fitted to a light microscope. (Inset): SEM image of an rbc-PtNPs-HALNN-ConA **1** aggregate acquired with the back-scattered electron detector.

attachment and an increase in polydispersity from 0.12 (PtNPs-HALNN) to 0.30 (PtNPs-HALNN-ConA **1**) (ESI, section 3). The zeta potential decreased from -35.1 mV (PtNPs-HALNN) to -27.6 mV (PtNPs-HALNN-ConA **1**) after ConA functionalisation. The formation of cross-linked clusters, whose size is dependent on the ratio of protein to PtNPs-HALNN, is expected, because both PtNPs-HALNN and ConA are multi-functional.[18] The synthesised PtNP-HALNN-ConA **1** clusters do not interact with plastic surfaces, can be freeze-dried from PBS buffer, stored long-term at -20 °C and simply reconstituted by resuspension in water using sonication.

With clusters PtNPs-HALNN-ConA **1** in hand, our attention turned to the rbc aggregation assay. Fresh rat blood was treated with the anticoagulant heparin, the erythrocytes were separated and resuspended in L-15 medium (Leibovitz) containing 0.2 mg/mL BSA. The freeze-dried sample ConA-HALNN-PtNPs **1** was resuspended in PBS containing Ca^{II}, Mg^{II} and BSA and added to the rbcs. The mixture was shaken at 100 rpm to induce shear forces for improved binding at 37 °C for 3 h (ESI, section 1.14). Samples were taken every 15 min and analysed using a light microscope. The ConA-modified clusters caused a strong agglutination whereas the negative controls, pure rbcs and rbcs mixed with PtNPs-HALNN, did not form any aggregates in the course of the experiment (**Fig. 3**). For scanning electron microscopy (SEM) analysis, the rbc-PtNPs-HALNN-ConA **1** aggregates were centrifuged, resuspended in 2.5% glutaraladehyde solution and the cells fixed at 5°C overnight. The fixative was decanted, the aggregates washed with PBS buffer solution and then one drop of the aggregate suspension was deposited on a cover slip coated with poly-L-lysine. The aqueous solution was replaced stepwise by ethanol and then the alcohol was removed from the specimen using a liquid CO_2 critical point dryer (ESI, section 1.15-1.16). **Fig. 3** (inset) and Fig. S3 (ESI) show SEM images of rbc aggregates made using the back-scattered electron (BSE) detector of the SEM. Heavy elements such as platinum back-scatter electrons more strongly than light elements and the PtNP-HALNN-ConA **1** clusters therefore appear very bright in the image. Fig. S4 (ESI) shows SEM images and EDS analysis of the rbc-bound PtNP-HALNN-ConA **1** clusters confirming the presence of platinum.

Next, the role of the concentration of the activating agents EDC/ sulfo-NHS and of ConA in the protein attachment step to the PtNPs-HALNN conjugates was investigated. PtNPs-HALNN conjugates were reacted with 270 µg of ConA without prior addition of coupling agents in an attempt to confirm whether the activation of the C-terminus of HALNN is required for ConA functionalisation. The generated clusters 2 had an average size of 374 nm (table 1 and ESI, section 3). The concentrations of EDC/ sulfo-NHS and ConA were then doubled compared to the initially used concentrations described in section 1.9 of the ESI yielding clusters 3 with an average size of 830 nm. A rbc aggregation assay was conducted as described in the ESI (section 1.14) using products 1-3. Clusters 3 clearly induced the strongest rbc aggregation, followed by compounds 1 and 2 confirming that the clusters that were larger in size led to increased rbc binding (ESI, Fig. S2). This assay demonstrated that ConA binds to the PtNPs-HALNN to a certain degree without activation of the C-terminus of HALNN, presumably *via* the interaction of lysine side-chains with the PtNP surface and hydrophobic/ hydrophilic interactions between the peptide and the protein. However, increasing the concentration of coupling agents and protein led to the attachment of more ConA to PtNPs-HALNN and to the formation of larger clusters. We envisage the size of the PtNPs-HALNN-protein clusters may be conveniently tuned by choosing the appropriate reaction time and ratio of concentration of protein to cross-linking groups (i.e. concentration of PtNPs-HALNN · number of active sites per NP).

Table 1 DLS size analysis of clusters PtNPs-HALNN-ConA **1-3**

PtNPs-HALNN-ConA	EDC*	Sulfo-NHS*	ConA [µg]	Z-Average [nm]**	PDI
1	6 eq.	1.5 eq.	270	427	0.30
2	-	-	270	374	0.25
3	12 eq.	3 eq.	540	830	0.31

* Relative to HALNN assuming 100% attachment to the PtNP surface
** After filtering through 0.45 µm syringe filters

Table 2 Characterisation data of precursor conjugates PtNPs-HALNN(E_6) and PEGylated and RGD-labelled PtNPs-HALNN(E_6) conjugates

Sample		Z-average before lyophilisation (nm)	PDI	Z-average after lyophilisation (nm)	PDI	Zeta potential mean (mV)	Zeta deviation (mV)
4	PtNPs-HALNN	37.8	0.12	153.9	0.36	-35.1	5.51
5	PtNPs-HALNNE$_6$	187.4	0.29	174.5	0.25	-37.3	7.36
6	PtNPs-HALNN-miniPEG	105.6	0.29	687.1	0.58	-22.6	7.96
7	PtNPs-HALNN-miniPEG-GRGD	82.1	0.23	648.7	0.90	-23.4	7.56
8	PtNPs-HALNNE$_6$-miniPEG	349.1	0.25	392.9	0.42	-29.5	10.80
9	PtNPs-HALNNE$_6$-miniPEG-GRGD	129.7	0.19	338.5	0.40	-27.5	11.3

Having established a robust procedure for the attachment of ConA to the PtNPs-HALNN conjugates, attention next turned to demonstrating that ConA can be replaced by other amine-containing ligands. H_2N-mini-PEG-CO_2H (ESI, section 1.4) was chosen as one of the ligands of interest since the covalent attachment of polyethylene glycol (PEG) to the PtNPs is expected to alter the size, polarity and surface properties of the PtNPs leading to changes in overall circulation life-span, tissue distribution pattern, and elimination pathway of the parent PtNP.[19] Another ligand studied was H_2N-mini-PEG-GRGD-CO_2H, a PEGylated RGD-peptide assembled *via* manual Fmoc SPPS on aminomethylated PS resin (ESI, section 1.5). The RGD motif is a minimal essential cell adhesion peptide sequence in fibronectin[20] with a high affinity for α_3, α_5, α_8, and α_v subunit integrin receptors present on a variety of cell types, including many tumour cells.[21] Both ligands were attached to freshly prepared samples of PtNPs-HALNN **4** and PtNPs-HALNNE$_6$ **5** conjugates (ESI, section 1.7 and 1.8) following a similar reaction procedure as developed for the attachment of ConA (ESI, section 1.10-1.13) giving rise to the PEGylated and RGD-labelled conjugates listed in **table 2**. Samples **6** and **7**, derived from the PtNPs-HALNN conjugate **4**, were small in size (106 and 82 nm, respectively) and relatively monodisperse before freeze-drying. After freeze-drying and redispersion in aqueous medium, however, their average size increased to 687 and 649 nm, respectively, and the samples were very polydisperse. The insertion of the E_6-tag again decreased aggregation. Samples **8** and **9** were 349 and 130 nm in size and relatively monodisperse before freeze-drying. After freeze-drying and resuspension, the size of **8** increased slightly to 393 nm and the size of **9** to 339 nm with a moderate increase in polydispersity (**table 2**). It was therefore decided to use only the E_6-tagged samples **5**, **8** and **9** in cell binding assays with S61 primary human fibroblasts and the murine pre-adipocyte 3T3-L1 cell line (ATCC® CL-173™). 3T3-L1 are known to express the RGD-binding $\alpha_v\beta_3$ integrin,[22] and S61 fibroblasts were shown to express both $\alpha_4\beta_1$ and $\alpha_5\beta_1$ integrins by flow cytometry (ESI, section 1.18 and Fig. S5). Both cell lines were grown to near confluency on glass slides in DF10 medium at 37°C; 5% CO_2 and then incubated overnight with one 200 uL aliquot each of **5**, **8** and **9** (ESI, section 1.19). Light microscopy images taken after 16 h of incubation time and after serial rinsing of the cells with PBS showed that **5** could easily be washed off both types of cell lines, whereas **8** and **9** stayed firmly attached to the cells (ESI, Fig. S6). The specimens were fixed and prepared for SEM imaging as described in section 1.20 of the ESI. The acquired SEM images are depicted in **Fig. 4** and Fig. S7 of the ESI. The images in **Fig. 4-a** (3T3-L1) and **Fig. 4-d** (S61) confirm a very low concentration of **5** in the specimens. The attachment of large amounts of **8** and **9** to the surfaces of the fibroblasts was confirmed by the images shown in **Fig. 4-b/c** (3T3-L1) and **Fig. 4-e/f** (S61), respectively.

Counts of PtNPs in SEM preparations per unit area (area 200 x 200 pixels; five counts per preparation) showed that in the case of the 3T3-L1 fibroblasts basically the entirety of **5** could be washed off by gently rinsing the cells with PBS (**table 3**). Moderate counts were detected for the PEGylated PtNPs **8** (64 ± 22) and the highest counts were obtained for RGD-labelled PtNPs **9** (124 ± 32), which is in accordance with the expected RGD-mediated adhesion to the $\alpha_v\beta_3$ and $\alpha_5\beta_1$ cell surface integrin receptors. In the case of the S61 fibroblasts, the counts for **8** and **9** were similar and both much higher than for **5**. A more complete investigation of differential integrin receptor expression by these cell lines may highlight binding preferences of RGD-labelled PtNPs to particular integrin heterodimers.

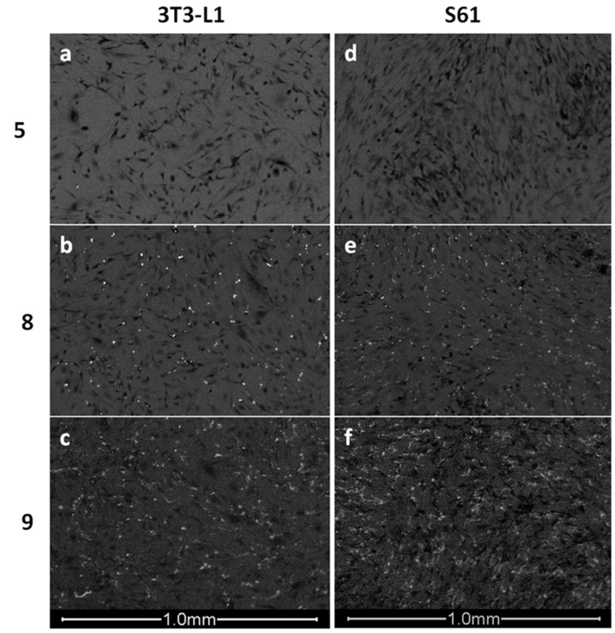

Fig. 4. Back-scattered electron SEM images of (a-c) 3T3-L1 and (d-f) S61 cells incubated with particles **5** (a,d), **8** (b,e) and **9** (c,f) No significant numbers of particles were found attached to the substrate.

Table 3 Number of PtNPs counted in the SEM specimens (mean ± SD)

Cells	PtNPs 5	PtNPs 8	PtNPs 9
3T3-L1	1 ± 1	64 ± 22	124 ± 32
S61	30 ± 12	417 ± 104	409 ± 119

Drug-carrying NPs are often PEGylated to enhance their aqueous solubility and circulation half-life.[23] It is assumed that PEG molecules provide a steric barrier for NPs, which could prevent the opsonisation of NPs by serum proteins[24] and suppress the wrapping of NPs by biomembranes.[25] However, our results and those of others suggest that PEGylated NPs can adhere to certain types of cells.[26] In this respect, highly negatively charged NPs such as the E_6-labelled PtNPs **5** may prove more advantageous. Interestingly, a significant difference between binding of PEGylated PtNPs **8** and RGD-labelled PEGylated PtNPs **9** was seen in 3T3-L1 cells, confirming that for certain cell types modulation of the NP surface groups can significantly alter their targeting behaviour.

In summary, we have developed a versatile synthesis protocol for the preparation of biologically targeted PtNPs which is transferable to the covalent attachment of a range of targeting ligands. The targeted PtNPs were accessible *via* a simple two-step procedure using peptides HALNN(E_6) as capping agents in the NP formation process and linkers to the targeting ligands. The attachment of the lectin ConA led to PtNPs that were targeted to the blood group antigens on the surface of rbcs and the size and biological activity of the PtNP-HALNN-ConA clusters could be tuned by adjusting the ratio of lectin to activated PtNP-HALNN species. The conjugation of a PEGylated RGD-peptide to the PtNPs yielded PtNPs that were targeted at $\alpha_v\beta_3$ and $\alpha_5\beta_1$ integrin receptors.

Acknowledgements

We thank the MacDiarmid Institute and the New Zealand MBIE for funding under contract C08X1003. The authors also wish to thank the patients who generously consented to the use of their tissue in this research, and acknowledge the assistance of a number of surgeons in obtaining that tissue, especially Ms. Michelle Locke.

Notes and references

[a] *The MacDiarmid Institute for Advanced Materials and Nanotechnology, School of Chemical Sciences, The University of Auckland, Private Bag 92019, Auckland 1123, New Zealand, E-Mail: m.brimble@auckland.ac.nz; david.williams@auckland.ac.nz.*

[b] *The MacDiarmid Institute for Advanced Materials and Nanotechnology, School of Chemical and Physical Sciences, Victoria University of Wellington, P.O. Box 600, New Zealand.*

[c] *School of Biological Sciences, The University of Auckland, Private Bag 92019, Auckland 1123, New Zealand*

† Electronic Supplementary Information (ESI) available: Experimental details, TEM, SEM and light microscope images, EDS analyses, SAED patterns, and DLS analyses. See DOI: 10.1039/c000000x/

1 (a) M. A. Khalily, O. Ustahuseyin, R. Garifullin, R. Genc, M. O. Guler, *Chem. Commun.*, 2012, **48**, 11358; (b) A. M. Henning, J. Watt, P. J. Miedziak, S. Cheong, M. Santonastaso, M. Song, Y. Takeda, A. I. Kirkland, S. H. Taylor, R. D. Tilley, *Angew. Chem. Int. Ed.,* 2013, **52**, 1477; (c) R. Bhandari, D. B. Pacardo, N. M. Bedford, R. R. Naik, M. R. Knecht, *J. Phys. Chem. C*, 2013, **117**, 18053.

2 (a) I. M. Rio-Echevarria, R. Tavano, V. Causin, E. Papini, F. Mancin, A. Moretto, *JACS,* 2011, **133**, 8; (b) M. Manikandan, N. Hasan, H.-F. Wu, *Biomaterials*, 2013, **34**, 5833; (c) N. Song, Y.-W. Yang, *Chem. Soc. Rev.*, 2015, DOI: 10.1039/c5cs00243e; (d) Y.-W. Yang, Y.-L. Sun, N. Song, *Acc. Chem. Res.*, 2014, **47**, 1950.

3 (a) S. Parveen, R. Misra, S. K. Sahoo, *Nanomed. Nanotech. Biol. Med.*, 2012, **8**, 147; (b) S. Cheong, P. Ferguson, K. W. Feindel, I. F. Hermans, P. T. Callaghan, C. Meyer, A. Slocombe, C.-H. Su, F.-Y. Cheng, C.-S. Yeh, B. Ingham, M. F. Toney, R. D. Tilley, *Angew. Chem. Int. Ed.*, 2011, **50**, 4206; (c) S. Cheong, P. Ferguson, I. F. Hermans, G. N. L. Jameson, S. Prabakar, D. A. J. Herman, R. D. Tilley, *ChemPlusChem*, 2012, **77**, 135.

4 (a) M. Shilo, T. Reuveni, M. Motiei, R. Popovtzer, *Nanomed.,* 2012, **7**, 257; (b) Z. Zhang, R. D. Ross, R. R. Roeder, *Nanoscale*, 2010, **2**, 582.

5 E. Porcel, S. Liehn, H. Remita, N. Usami, K. Kobayashi, Y. Furusawa, C. Le Sech, S. Lacombe, *Nanotechnology*, 2010, **21**, 085103.

6 Y. Teow, S. Valiyaveettil, *Nanoscale*, 2010, **2**, 2607.

7 W.-K. Kim, J.-C. Kim, H.-Y. Park, O.-J. Sul, M.-H. Lee, J.-S. Kim, H.-S. Choi, *Exp. Mol. Med.*, 2012, **44**, 432.

8 (a) A. Watanabe, M. Kajita, J. Kim, A. Kanayama, K. Takahashi, T. Mashino, Y. Miyamoto, *Nanotechnology*, 2009, **20**, 455105; (b) M. U. Rehmann, Y. Yoshihisa, Y. Miyamoto, T. Shimizu, *Inflammation Research*, 2012, **61**, 1177.

9 P. V. Asharani, N. Xinyi, M. Prakash Hande, S. Saliyaveettil, *Nanomed.*, 2010, **5**, 51.

10 (a) L. M. Forbes, A. P. Goodwin, J. N. Cha, *Chem. Mater.*, 2010, **22**, 6524; (b) L. Ruan, C.-Y. Chiu, Y. Li, Y. Huang, *Nano Letters*, 2011, **11**, 3040; (c) Y. Li, G. P. Whyburn, Y. Huang, *JACS*, 2009, **131**, 15998; (d) C.-Y. Chiu, Y. Li, L. Ruan, X. Ye, C. B. Murray, Y. Huang, *Nature Chemistry*, 2011, **3**, 393.

11 (a) D. S. Sheny, D. Philip, J. Mathew, *Spectrochim. Acta A*, 2013, **114**, 267; (b) A. Syed, A. Ahmad, *Colloids Surf., B*, 2012, **97**, 27; (c) A. Senuga, J. Van Marwijk, A. Boshoff, C. G. Whiteley, 2012, 14, 824; (d) B. H. San, S. H. Moh, K. K. Kim, *J. Mater. Chem.*, 2012, **22**, 1774; (e) J. Kim, T. Shirasawa, Y. Miyamoto, *Biomaterials*, 2010, **31**, 5849.

12 V. Gubala, C. Crean, R. Nooney, S. Hearty, B. McDonnell, L. Heydon, R. O'Kennedy, B. D. MacCraith, D. E. Williams, *Analyst*, 2011, **136**, 2533.

13 R. Lévy, N. T. K. Thanh, R. C. Doty, I. Hussain, R. J. Nichols, D. J. Schiffrin, M. Brust, D. G. Fernig, *JACS*, 2004**, 126**, 10076.

14 (a) L. Kumar, N. R. Kandasamy, T. S. Srivastava, A. J. Amonkar, M. K. Advankar, M. P. Chitnis, *J. Inorg. Biochem.*, 1985, **23**, 1; (b) E. M. A. Ratilla, H. M. Brothers II, N. M. Kostić, *JACS*, 1987, **109**, 4592; (c) A. Carlsen, S. Higashiya, N. I. Topilina, K. A. Dunn, R. E. Geer, E. T. Eisenbraun, A. E. Kaloyeros, J. T. Welch, *Macromol. Biosci.*, 2012, **12**, 269.

15 J. M. Slocik and D. W. Wright, *Biomacromolecules,* 2003**, 4**, 1135

16 F. Albericio, R. Van Abel, G. Barany, *Int. J. Peptide Protein Res.*,1990, **35**, 284.

17 A. E. Clarke, M. A. Denborough, *Biochem. J.*, 1971, **121**, 811.

18 S. Connolly, S. Cobbe, D. Fitzmaurice, *J. Phys. Chem. B*, 2001, **105**, 2222.

19 M. Hamidi, A. Azadi, P. Rafiei, *Drug Deliv.*, 2006, **13**, 399.

20 M. D. Pierschenbacher, E. Ruoslahti, *Nature*, 1984, **309**, 30.

21 (a) E. F. Plow, T. A. Haas, L. Zhang, J. Loftus, J. W. Smith, *J. Biolog. Chem.*, 2000, **275**(29), 21785; (b) U. Hersel, C. Dahmen, H. Kessler, *Biomaterials*, 2003, **24**, 4385.

22 H. Sekimoto, J. Eipper-Mains, S. Pond-Tor, C. M. Boney, *Molecular Endocrinology*, 2005, **19**(7), 1859.

23 (a) Y. Li, Y. Hu, *RSC Adv.*, 2014, **4**, 51022; (b) P. Calleja, S. Espuelas, C. Vauthier, G. Ponchel, J. M. Irache, *J. Pharm. Sci.*, 2015, DOI: 10.1002/jps.24354 (ahead of print).

24 D. E. Owens 3rd, N. A. Peppas, *Int. J. Pharm.*, 2006, **307**(1), 93.

25 M. Schulz, A. Olubummo, W. H. Binder, *Soft Matter*, 2012, **8**, 4849.

26 H. S. Huang, J. F. Hainfeld, *Int. J. Nanomed.*, 2013, **8**, 2521.